Sensors and Materials, Vol. 9, No. 2 (1997) 107–116
MYU Tokyo

S & M 0277

Current-Voltage Characteristics of Thin Film SnO_2 Gas Sensors: Electronic Artifacts and Gas Response

Georg Steimer, Gerd Sulz, Gerd Kühner, Helmut Reiter, Ulrich Hoefer* and Klaus Steiner**

Fraunhofer-Institut für Physikalische Meßtechnik, Heidenhofstr. 8, D-79110 Freiburg, Germany

(Received November 28, 1995; accepted August 26, 1996)

Key words: SnO_2, gas sensor, platinum, contact area, IV characteristic

Current-voltage characteristics of implanted thin film SnO_2 gas sensors are measured in various gas atmospheres. The gas-sensitive SnO_2 layers are contacted with Pt electrodes. The metal semiconductor contacts show poor rectifying characteristics. Pd-, Pt-, Sb-, In-, Ni- and Ca-implanted sensors are investigated. Gas response and signal drift are strongly dependent on the sensor current-voltage operating point. Depending on the bias voltage artifacts which seriously distort gas response pattern can be produced. CO, CO_2, NH_3, NO_2 and CH_4 responses in humid air are discussed.

1. Introduction

Optimization of metal-oxide gas sensors and sensor arrays has mainly concentrated on the sensitive sheet itself. Investigations have been made on morphology, defects, dopants, operating temperature, atomistic models for molecular recognition, electrical measurement and preparation conditions.[1] Recently, it has become apparent through engineering of SnO_2 thin-film gas sensors, that a systematic investigation of the contact area between the electrodes and the sensitive layers is required.[2] Scaling the contact area enhances gas response towards specific gases. In this work we concentrate on Pt contacts to doped SnO_2,

*Author to whom correspondence should be addressed.
**New address: Ruhrgas Industrie Beteiligungs GmbH, D-45138 Essen, Huttropstr. 60, Germany.

since such contacts are widely used. Current-voltage characteristics of such interfaces are measured in various gas atmospheres. Electronic artifacts and gas responses are discussed.

2. Sensor Preparation

A top view of the investigated sensor elements is shown in Fig. 1. The devices were structured on standard 4-inch Si substrates using conventional thin film technology. The Si substrates were covered by a 1-μm-thick SiO_2 layer for electrical insulation of the substrate from the electrodes and sensitive layers. Pt electrodes and Pt heater were sputtered directly onto photolithographic patterns. Definition of the structures was accomplished by lift-off. The 50-nm-thick SnO_2 layers were selectively sputtered onto the Pt electrodes using a photoresist mask. The deposition was performed in Ar/O_2 gas mixture at 0.5 kW with a total gas flow of nearly 3 sccm in a Leybold Z550 r.f. sputtering system. Pd, Pt, Sb, In, Ca and Ni dopants were implanted. To activate the implants and to stabilize the sensitive layers, the wafers were subjected to rapid thermal annealing in synthetic air for 30 min at 700°C. For measurements, elements were mounted into TO-5 packages.

The power consumption was 0.6–1.4 W between 100 and 350°C. Using a sensor on a SiOxNy membrane, power consumption could be lowered to 0.1–0.4 W. The membrane technology had no influence on the gas response. Details of the fabrication and implantation process are discussed elsewhere.[3, 4]

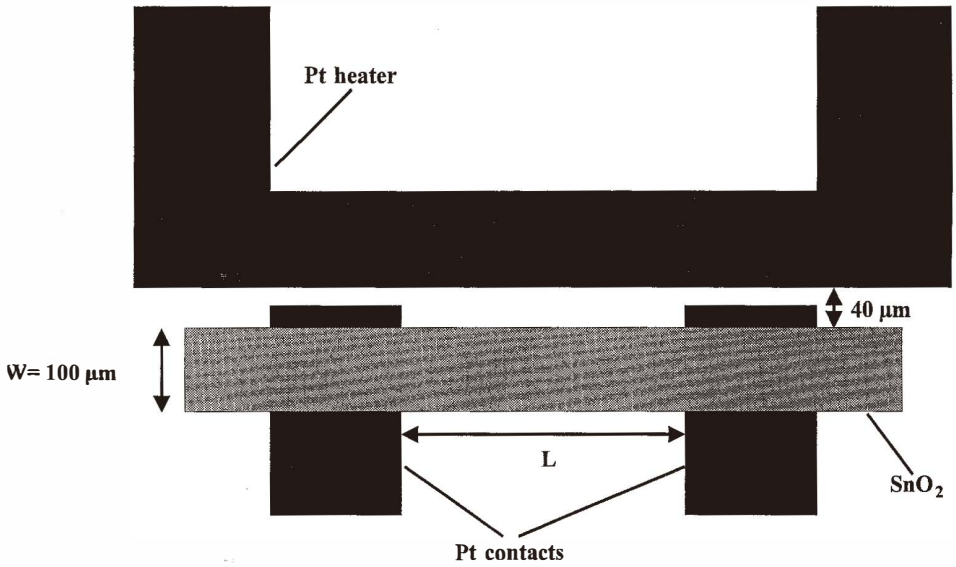

Fig. 1. Top view of investigated SnO_2 sensors. Contact separation L1 = 10 μm, L2 = 500 μm.

3. Gas Measurements

The gas sensors were tested in humid, synthetic air. Additionally, commercially available test gases such as CO, CO_2, NH_3, NO_2 and CH_4 were used. The flow rate was always 1 slm (standard liter per minute). The gas stream direction and the sensor surface were parallel. During operation, current-voltage (IV) characteristics were measured once every 5 min using a Hewlett-Packard semiconductor parameter analyzer (HP 4145 B). To prevent line-frequency interference and other noise sources from affecting the accuracy of measurements, the digital integration time is typically set to "long" and the measurement result is the average value of 256 samples taken within each measurement cycle. To show trapping effects the digital integration time was set to "medium." In this case a total of 16 samples were taken for each measurement cycle. The integration time lasts almost 20 and 320 ms, respectively.[5] To prove reproducibility of the results several devices of each wafer were measured. Moreover, results were rechecked by measurements on different wafers. The voltage range was limited to +10 V to prevent damage and irreversible changes of the structure by high currents.

Figure 2 shows gas-sensitive current-voltage characteristics of a Pt-SnO_2-Pt system. The IV- curves were modulated by 1000 ppm CH_4, 40 ppm NO_2, 100 ppm NH_3 and 2500 ppm CO_2. Pt-SnO_2 and SnO_2-Pt contacts were switched in series. Thus the system was comparable to a MSM structure (metal-semiconductor-metal diode[6]). During sensing, one of the two contacts was forward-biased and the other one was reverse-biased. Figure 2 shows some basic features which should be highlighted. First, since leakage currents are high, the characteristics demonstrate poor rectifying properties of both Pt-SnO_2 contacts. Reactance contributions can be expected.[7] Since IV curves are not symmetrical, the rectifying behavior of both contacts is slightly different. Contributions from the sensitive layer seem to be minor.[2, 7] Close to –10 V bias voltage breakdown of one contact arises. This cannot be seen at +10 V bias. However, breakdown can be expected at higher voltages.

The IV response is strongly influenced by the gas flowing past the sensor. The IV curves are mainly modified at high and low bias voltages ($> +5$ V and < -5 V). As expected in this bias voltage range, reducing gases such as CH_4 and NH_3 increase the current, while oxidizing gases such as NO_2 decrease it.[8] Between +2 and +4 V bias voltages the IV characteristics exhibit a current peak. Such a current peak usually appears in tunneling devices.[6] In this region reducing gases such as CH_4 can shift the current below the reference value taken in humid synthetic air. Thus, in this case a reducing gas reduces the current, which is in contrast to the expectations in the literature.[8] The sensor signal change then becomes dependent on the operating voltage. It is assumed here that this phenomenon is mainly caused by an electronic effect, since the gas influence has been the same over the entire voltage range. Such electronic mechanisms can produce a unique sensor behavior, which is discussed later in more detail. The occurrence of such peak currents is independent of the contact separation L and width W of the sensitive sheet. However, L produces an SnO_2 sheet resistance which as series resistance limits the total current. The current peaks are shifted to higher voltages (see also Fig. 3). Peak currents were also observed at negative bias voltages. Although the contacts are geometrically

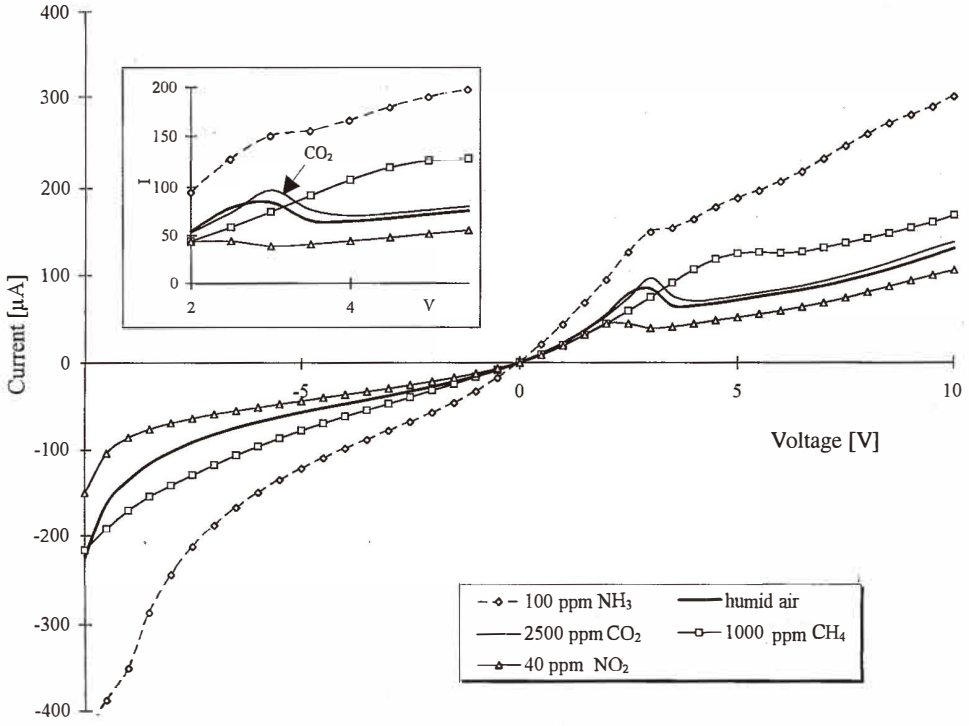

Fig. 2. Current-voltage characteristics of a thin film Pd-implanted SnO_2 sensor. Dosage: 2.5×10^{15} cm^{-2}, acceleration voltage: 60 kV, characteristics modulated by 40 ppm NO_2, 1000 ppm CH_4, 100 ppm NH_3 and 2500 ppm CO_2, contact separation 10μm, operating temperature 300°C, humid air, 50% r. h. (23°C reference temperature). Inset shows magnified current peaks around +3 V bias voltage, measurement time tm: "long" tmm = 320 ms.

identical and structured simultaneously, it is important to note that asymmetrical IV characteristics occurred. The two contacts do not necessarily exhibit similar electrical characteristics. Therefore, a plot of symmetrical IV characteristics is not shown here.

As expected, CO_2 has nearly no influence on the sensor current. IV curves modulated by CO_2 and humid synthetic air are almost identical. Only close to the current peak around +3 V might there be some differences (see also arrow in inset of Fig. 2). There, the current shift is more pronounced than that observed in Ref. 9. Thus, using a special IV behavior, CO_2 might be, in principle, detectable in a distinct voltage range. This simply shows that a special interface configuration might be important for CO_2 detection with SnO_2 sensors.

The current peaks are dependent on the measurement time, as shown in Fig. 3. There, a "medium" (~ 50 ms) and a "long" (~ 320 ms) integration time were selected. Differences between the two sets of curves are obvious. In particular, the peak currents are heavily

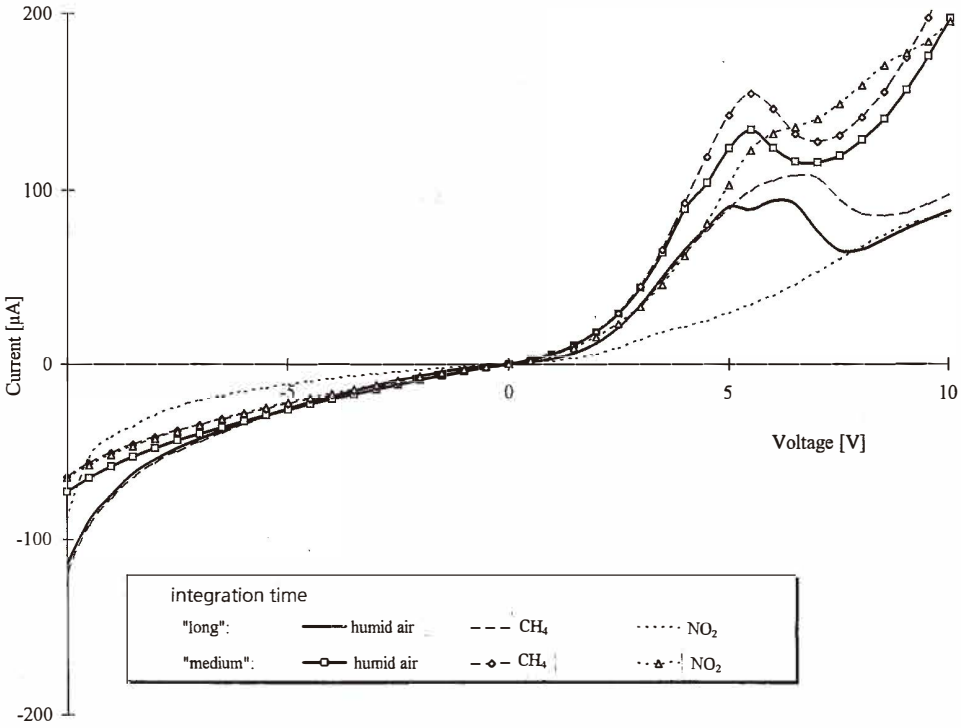

Fig. 3. Current-voltage characteristics of a thin film Pd-implanted SnO_2 sensor. Dosage: 2.5×10^{15} cm^{-2}, acceleration voltage: 60 kV, characteristics modulated by 40 ppm NO_2 and 1000 ppm CH_4, contact separation 10 μm, operating temperature 300°C, humid air, 50% r. h. (23°C reference temperature), measurement time tm: "medium" tmm = 20 ms and "long" tml = 320 ms.

enhanced. Currents dependent on the measurement time can be typically observed in semiconductors with a high concentration of deep levels.[10] In this work, such effects seem to be modulated by gas response.

From gas-modulated IV curves, sensor sensitivities can be evaluated. In Fig. 4, NO_2 sensitivities are given with the total bias voltage as a parameter. The sensitivity is the measured current I divided by the reference current Io measured at t = 0 s in humid synthetic air. For a better overview, only the positive range of voltages was used for the evaluations. The field of sensitivity curves does not show a common tendency. The sensitivity increases and decreases as well. It is quite obvious that the nonlinear IV characteristics lead to bias-voltage-dependent sensitivities. Moreover, long-term stabilities are heavily degraded with increasing total sensor current.

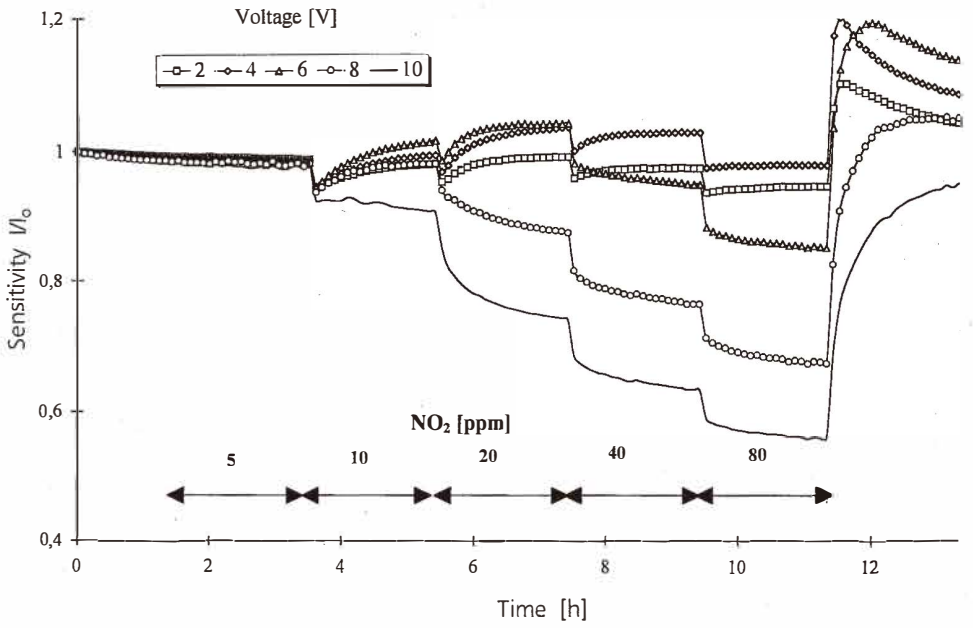

Fig. 4. NO_2 sensitivity of a thin film In-implanted SnO_2 sensor at different bias voltages. Dosage: 5×10^{15} cm^{-2}, acceleration voltage: 60 kV, characteristics modulated by 5, 10, 20, 40 and 80 ppm NO_2, contact separation 10 μm, operating temperature 300°C, humid air, 50% r. h. (23°C reference temperature), current reference values Io: 2 V: Io2V = 0.17 μA, 4 V: Io4V = 0.35 μA, 6 V: Io6V = 0.58 μA, 8 V: Io8V = 0.82 μA, 10 V: Io10V = 1.01 μA, measurement time tm: "long" tmm = 320 ms.

4. Discussion

Charge transfer from reacting species and molecules to the sensor can lead to a change in the free charge concentration inside the sensitive layer, resulting in conductivity modulations. However, conductivity can also be changed by pure electronic effects such as free charge trapping, carrier injection at forward-biased rectifying contacts, tunneling and barrier-limited conduction.[6] Moreover, such electronic-induced effects can influence the distribution of the free carrier density and therefore, finally, gas reactions. Since charge transfer caused by gas reactions and charge modulation caused by electronic effects can hardly be separated, any conductivity modulation is usually interpreted as a gas response. Recently, some electronic effects such as contact influences, however, were investigated in more detail.[2, 11, 12] It has been pointed out that contacts with poor rectifying properties have a significant influence on sensor response. Moreover, systematically changing Schottky barriers by changing the contact area leads to a tool for enhancing sensitivity towards specific gases. So far, such investigations have been mainly concentrated on Pt-SnO_2 contacts.

Pt is widely used as an electrode material since Pt-SnO_2 interfaces lead to temperature-stable contacts with poor rectifying properties.[9] Interface degradations by interdiffusion are limited to a few nm. However, Pt diffusion into SnO_2 cannot be totally suppressed. This creates a region of a SnO_2 matrix with a high content of Pt. In Ref. 2 this layer is called a modified sheet. Usually only a few atomic layers are necessary to establish interface potential barriers.[13] Thus, this region limits electrical interface properties. Moreover, the modified sheet produces most of the signal contributions to the total sensor gas response. This is particularly true for oxidizing gases like NO_2.[2] With improvement of rectifying properties, NO_2 sensitivity will be optimized. For mass production this interface region needs to be controlled more carefully to exclude inhomogeneities across the wafers. This point will be discussed later in more detail.

The asymmetric IV characteristics in Fig. 2 show that geometrically identical and simultaneously produced Pt-SnO_2 contacts do exhibit different interface properties. Additionally, contact inhomogeneities can be observed by scanning IV characteristics across a wafer and from wafer to wafer (not shown here). At some points, current peaks occur which might be caused by tunneling effects. Inhomogeneities are very much pronounced with Ni, Pt and Ca implants. Fluctuations can be limited by implanting Sb, In and Pd dopants. The influences of these dopants are not yet clear. However, it is assumed here that interface interdiffusion might be limited by special dopants. It is therefore proposed in this work to investigate this in more detail by introducing temperature-stable interfacial layers.

The current peaks in Figs. 2 and 3 seem to be caused by trap-assisted tunneling, since the currents are strongly dependent on the measurement time. The currents decrease with increasing digital integration time. Thus charge losses occur. One reason for this might be the acceptor-like states. Since the above-mentioned effects are strong only at and above the current peak voltage, acceptor states close to the Pt-SnO_2 interfaces seem to play a major role. Band bending at the rectifying contacts shifts the states close to the Fermi level and allows charging of the level. Further electron losses, however, for instance due to NO_2 reaction, suppress the influence of such states. Charging thus becomes less probable and no longer contributes to the current drift. Moreover, band bending suppresses trap-assisted tunneling and current peaks disappear. Pd dopants lead to acceptor-like bulk states.[11,12] However, it seems to be somewhat speculative to conclude any influence of Pd on the effects observed in Fig. 3. This is also underlined by measurements of samples with different metallic implants. There, similar observations were made. To clarify this in more detail, temperature-dependent trap analysis with gas influence is necessary.

The question of how to measure sensitivity of such gas sensors arises. Around the current peaks, conductivity measurements for sensitivity evaluations are not recommended because there the conductivity is strongly voltage-dependent. Simple gas modulation can shift the operation point from the right to the left side of the current peaks or vice versa. Moreover, even "negative" conductivity values can be measured. Thus, electronic effects distort gas response. Current measurements at constant voltages might also lead to unique results. This is illustrated in Fig. 4. All the evaluations give misleading results. By measuring the IV characteristics, however, such artifacts can be clarified. In this work only the nonlinear IV curves cause voltage-dependent sensitivities. No difficult chemical

reactions need to be taken into account.[14] In particular, this is true for the NO_2 response. From the above results one can conclude that only by IV measurements can such sensitivity artifacts be clarified. Following this step, the optimal potential range can then be selected where conductance and/or current information for sensitivity evaluations should be measured. As long as sensor behavior across a wafer and from wafer to wafer show such interface inhomogeneities, IV-curves need to be measured first to suppress electronic artifacts.

Interface properties are dependent on the operating temperature. Usually, rectifying properties of Schottky barriers are degraded with increasing temperature. Differences between the electronic properties of metal-semiconductor interfaces will change with the temperature. However, they do not vanish totally over the selected temperature range. In particular, this holds for wide band-gap materials. Since free charge generation occurs at high temperatures, investigations of electronic interface properties at low temperatures might be advantageous. For instance, higher free charge densities mask the Coulomb scattering of defects at interfaces more effectively. Thus, room temperature measurements are a convenient tool for detecting electronic interface inhomogeneities across a wafer and from wafer to wafer. For on-wafer mapping, conventional microelectronic probe card systems can be used.

Figure 5 shows IV characteristics of sensors measured at room temperature and the related high-temperature gas response pattern. The sensor chips were taken from neighboring cells of one wafer. The upper and lower set of curves were measured on sensors with a contact separation of L = 10 μm and L = 500 μm, respectively. It is obvious that the lower set of curves lie closer together than the upper one. Scattering is less pronounced and inhomogeneities are limited. From Fig. 5 we conclude the following two points: firstly, the higher sheet resistances of larger contact separations limit the formation of inhomogeneities. This is true for room temperature as well as for operating temperatures. Secondly, contact resistances are much more inhomogeneous than sheet resistances. This result was confirmed by Transmission Line Method (TLM) measurements (not shown here).[2] Sheet resistances are much more homogeneous across a wafer and from wafer to wafer than the contact resistances. This is true for structures with dimensions less than 0.5 mm. However, sensitive sheets with contact separations longer than 0.5 mm (width 100 μm) exhibit stronger fluctuations of the sheet resistances. Thus, optimized scaling leads to dimensions less than 0.5 mm. Optimization of gas sensors should focus on improvements of homogeneity of Pt-SnO_2 contact interfaces in such structures.

5. Conclusion

Electrical measurements of gas concentrations with SnO_2 sensors require a systematic investigation of the current-voltage characteristics. Such investigations lead to an optimal electrical operation point for sensing. Otherwise, electronic artifacts cannot be observed and effectively excluded, and therefore sensitivity evaluations might be heavily distorted. Such electronic artifacts are mainly caused by the gas-sensitive nonlinear current-voltage characteristics of Pt-contacted SnO_2 sensors. Inhomogeneities of sensor properties across

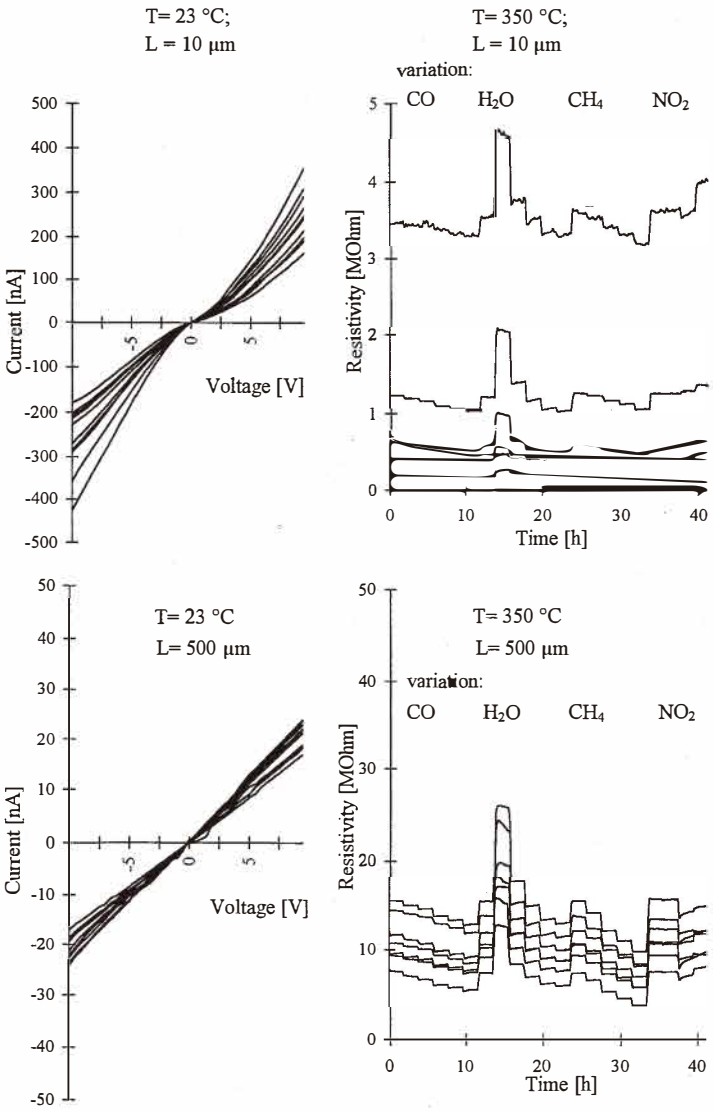

Fig. 5. Current-voltage characteristics at room temperature and high-temperature CO, H_2O, CH_4 and NO_2 response of In-implanted SnO_2 sensors in humid synthetic air. Dosage: 5×10^{15} cm^{-2}, acceleration voltage: 60 kV, characteristics modulated by 5, 10, 30, 50 and 100 ppm CO (50% r.h.), 10, 30, 50, 70 and 80% rel. humidity (23°C reference temperature), 100, 500, 1000 and 2000 ppm CH_4 (50% r. h.) and 5, 10 and 20 ppm NO_2 (50% r. h.), measurement time tm: "long" tmm = 320 ms.

a wafer are mainly caused by scattering of the electronic interface properties. Wafer mapping of current-voltage characteristics at room temperature provides a tool for reviewing scattering of high-temperature gas response across a wafer. To exclude scattering of sheet resistance values, optimal contact separation should be less than 0.5 mm (SnO_2 width W = 100 μm). In that case, sensor optimization procedures can focus on the contact interfaces and the preparation conditions.

References

1 W. Göpel and K. D. Schierbaum: Sensors and Actuators **B26-B27** (1995) 1.
2 U. Hoefer, K. Steiner and E. Wagner: Sensors and Actuators **B26-B27** (1995) 59.
3 K. Steiner, U. Hoefer, G. Kühner, G. Sulz and E. Wagner: Thin-film SnO_2 Gas Sensors on Si Substrates for CO and CO_2 Detection, Microsystem Technologies '94, 4th International Conference on Micromechanical Systems and Components, Berlin, FRG, October 19-21, 1994, Eds.. H. Reichl and A. Heuberger (VDE-Verlag, Berlin 1994) p. 429.
4 G. Sulz, G. Kühner, H. Reiter, G. Uptmoor, W. Schweizer, H. Löw, M. Lacher and K. Steiner: Sensors and Actuators **B15-B16** (1993) 390.
5 Hewlett-Packard: HP 4145 B Operation Manual (1986) Section III, page 3.
6 S.M. Sze: Physics of Semiconductor Devices (John Wiley & Sons, New York, 1981).
7 U. Weimar and W. Göpel: Sensors and Actuators **B26-B27** (1995) 13.
8 D. Kohl: Sensor and Actuators **18** (1989) 71.
9 U. Hoefer, G. Kühner, W. Schweizer, G. Sulz and K. Steiner: Sensors and Actuators **B22** (1994) 115.
10 A. K. Jonscher: Solid-State Electronics **33**(1) (1990) 139.
11 K. D. Schierbaum, J. Geiger, U. Weimar and W. Göpel: Sensors and Actuators **B13-B14** (1993) 143.
12 K. D. Schierbaum, U. K. Kirner, J. F. Geiger and W. Göpel: Sensors and Actuators **B4** (1991) 87.
13 W. Mönch: Semiconductor Surfaces and Interfaces, Springer Series in Surface Sciences 26 (Springer-Verlag, Berlin, 1993) Chap. 19
14 G. Williams and G. S. V. Coles: Sensors and Actuators **B15-B16** (1993) 349.